Epidermal Basement Membrane Substitutes for Bioengineering of Human Epidermal Equivalents

Nikola Kolundzic[1,2,5], Preeti Khurana[1,2,5], Debra Crumrine[3,4], Anna Celli[3,4], Theodora M. Mauro[3,4] and Dusko Ilic[1,2]

Epidermal basement membrane, a tightly packed network of extracellular matrix (ECM) components, is a source of physical, chemical, and biological factors required for the structural and functional homeostasis of the epidermis. Variations within the ECM create distinct environments, which can affect the property of cells in the basal layer of the epidermis and subsequently affect keratinocyte differentiation and stratification. Very little attention has been paid to mimicking basement membrane in organotypic cultures. In this study, using parameters outlined in a consensus on the quality standard of organotypic models suitable for dermatological research, we have evaluated three basement membrane substitutes. We compared fibronectin with three complex three-dimensional matrices: Matrigel, decellularized dermal fibroblast–produced and –assembled ECM, and a dry human amniotic membrane. Our results suggest that Matrigel is not a suitable substrate for human epidermal equivalent culture, whereas the two other complex three-dimensional substitutes, decellularized dermal fibroblast–produced and –assembled ECM and dry human amniotic membrane, were superior to single layer fibronectin coating. Human epidermal equivalents cultured on either decellularized dermal fibroblast–produced and –assembled ECM or on dry human amniotic membrane generated hemidesmosomes, whereas those on fibronectin did not. In addition, human epidermal equivalent cultured on decellularized dermal fibroblast–produced and –assembled ECM and on dry human amniotic membrane can be maintained in culture 4 days longer than human epidermal equivalent cultured on fibronectin without compromising the barrier function.

INTRODUCTION

Epidermal basement membrane, comprised of an extensive network of extracellular matrix (ECM) components, plays multiple complex roles in maintaining epidermal homeostasis. The core components and central organizers of the basement membrane are laminins, which together with collagen IV and heparan sulfate proteoglycans form an intricate, tightly packed mesh. Various GFs, morphogens, and other regulatory macromolecules tethered to basement membrane constituents provide the signals involved in governing keratinocyte (KC) adhesion, differentiation,

stratification, and survival (Pozzi et al., 2017; Randles et al., 2017; Roig-Rosello and Rousselle, 2020). Mutations in ECM constituents are often associated with devastating diseases such as junctional or recessive dystrophic epidermolysis bullosa.

Various strategies have been used to mimic the complexity of the basement membrane in the bioengineering of organotypic cultures (Cruz-Acuna and Garcia, 2017; Zhang et al., 2021). However, for the bioengineering of human epidermal equivalents (HEEs), in most cases, the KCs are plated on a surface coated with a single ECM component such as fibronectin or collagen I (Khurana et al., 2021). Although HEEs generated in such a way resemble epidermis morphologically and functionally, they can be maintained in the culture only for 2–3 days before they start to deteriorate.

The discovery of more suitable basement membrane substitutes that can better support the structural and functional integrity of HEEs in a simple model will allow for further studies on epidermal homeostasis and the biology of the dermal–epidermal junction and for a better understanding of how dysfunction of these components leads to diseases.

It is plausible to hypothesize that more precise mimicking of the basement membrane in vitro might provide the signals that would support longer survival of the HEE. However, despite recent technical advances, full characterization of spatio–temporal expression of the constituents is still a major challenge. Bioengineering a basement membrane in vitro from single constituents would be nearly impossible owing to the complexity of the structure required; we have therefore compared three different approaches to mimic the

[1]Department of Women & Children's Health, School of Life Course & Population Sciences, Faculty of Life Sciences & Medicine, King's College London, London, United Kingdom; [2]Assisted Conception Unit (ACU), Guy's and St Thomas' NHS Foundation Trust, London, United Kingdom; [3]UCSF Department of Dermatology, University of California San Francisco, San Francisco, California, USA; and [4]San Francisco Veteran Affairs Medical Center, San Francisco, California, USA

[5]These authors contributed equally to this work.

Correspondence: Dusko Ilic, Assisted Conception Unit (ACU), Guy's and St Thomas' NHS Foundation Trust, 11th Floor, Tower Wing, London SE1 9RT, United Kingdom. E-mail: dusko.ilic@kcl.ac.uk

three-dimensional (3D) structure of the basement membrane in vitro: (i) Matrigel, (ii) decellularized dermal fibroblast–produced and –assembled ECM (dDF ECM), and (iii) commercially available dry human amniotic membrane (dHAM).

Matrigel is a protein mixture secreted by Engelbreth-Holm-Swarm mouse sarcoma cells. According to the manufacturer (Corning, Corning, NY), Matrigel is approximately 60% laminin, 30% collagen IV, and 8% entactin. Entactin interacts with both laminin and collagen IV and contributes to the 3D assembly of these ECM constituents. It also contains heparan sulfate proteoglycans and various GFs (i.e., IGF1, TGFβ1, EGF, PDGF, FGF2, NGF, and VEGF). Matrigel resembles the complex ECM composition found in many tissues and is used as a substrate for culturing cells and organoid development (Borries et al., 2020).

We have previously used native decellularized dermal fibroblast ECM as a substrate for the culture of pluripotent stem cell lines under xeno-free conditions (Ilic et al., 2012). Although it does not precisely mimic the basement membrane, dDF ECM contains a combination of ECM constituents that may contribute to its formation (Zhang et al., 2021).

Human amniotic membrane is a 20–500-µm thick, avascular structure. The epithelium, a single layer of cuboidal cells, faces the amniotic fluid. Underlying the epithelium is a basement membrane, which consists mainly of collagens and laminins. The basement membrane also contains soluble factors that are associated with anti-inflammatory effects and are responsible for regulating proliferation, migration, and differentiation of neighboring epithelial cells (Bourne, 1960; Gindraux et al., 2013; van Herendael et al., 1978). Under the basement membrane are the mesoderm layers, consisting of an acellular compact layer, a fibroblastic layer containing a netting of mesenchymal stromal/stem cells, and a spongy layer that is rich in proteoglycans and glycoproteins. Numerous studies have revealed the presence of multiple GFs in the human amniotic membranes (Dietrich-Ntoukas et al., 2012; Koizumi et al., 2000; Koob et al., 2014). Dehydration, lyophilization, and cryopreservation techniques, each with individual advantages and disadvantages, have been used for the preservation of commercial human amniotic membrane products. In this study, we chose to test dehydrated/dHAM because it can be stored at room temperature for months or even years (Ilic et al., 2016).

In this study, we compared the morphological and functional characteristics of human skin with HEE grown either on a fibronectin-coated surface or on 3D basement membrane substitutes: dDF ECM and dHAM (Figure 1). To validate our HEEs grown on different substrates, we followed the parameters outlined in a consensus for the quality standard of organotypic models suitable for dermatological research (van den Bogard et al., 2021).

RESULTS

Matrigel is not a suitable basement membrane substitute for bioengineering HEEs

We first investigated whether the HEE grown on different substrates can form an epidermal permeability barrier, using transepithelial electrical resistance (TEER) as a parameter (Uchida and Celli, 2020). Expected results were in the range
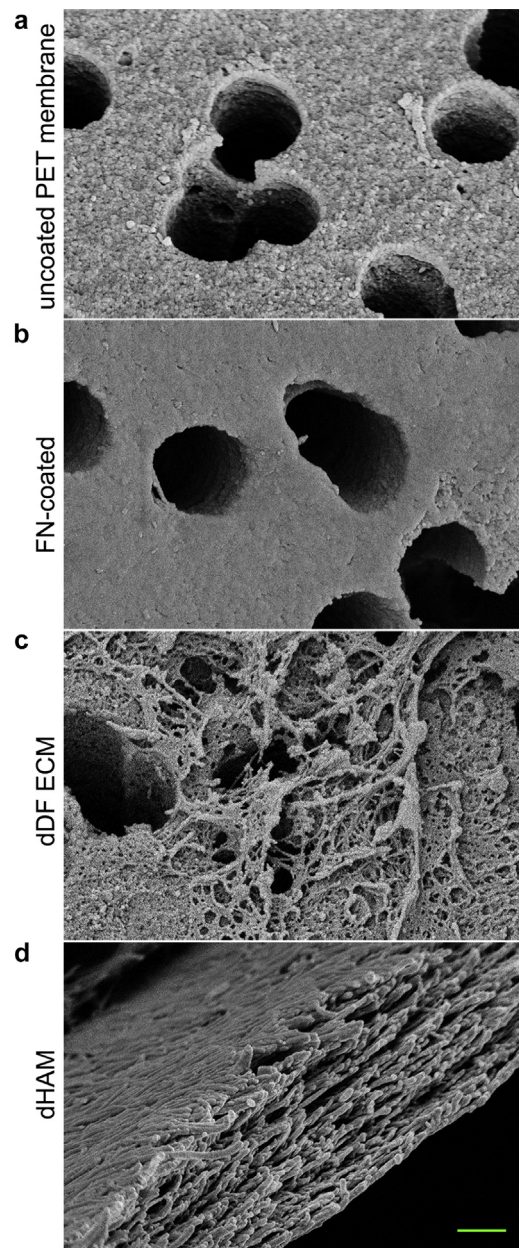
Figure 1. SEM images of epidermal basement membrane substitutes used for bioengineering of HEEs. (**a**) Uncoated PET membrane of Transwell inserts. (**b**) FN-coated PET membrane, (**c**) dDF ECM, and (**d**) dHAM used as a substrate for growing HEEs. Bar = 200 nm. dDF ECM, decellularized dermal fibroblast–produced and –assembled extracellular matrix; dHAM, dry human amniotic membrane; FN, fibronectin; HEE, human epidermal equivalent; PET, polyethylene terephthalate; SEM, scanning electron microscopy.

of $1,200–2,500\ \Omega cm^2$ (van den Bogard et al., 2021). HHEs cultured on various concentration of Matrigel (5.0, 2.5, 1.0, 0.5, and 0.1 mg/ml) were unable to stratify (data not shown). The maximum TEER achieved was between 800 and 1,000 Ωcm^2. H&E staining confirmed that HEEs cultured on Matrigel had no proper stratification of epidermal layers; no further characterization was therefore carried out.

Two other substitutes, dDF ECM and dHAM, performed better than fibronectin, which we were using previously (Petrova et al., 2016, 2014; Sun et al., 2015). HEE grown on fibronectin-coated surface could maintain TEER in the range
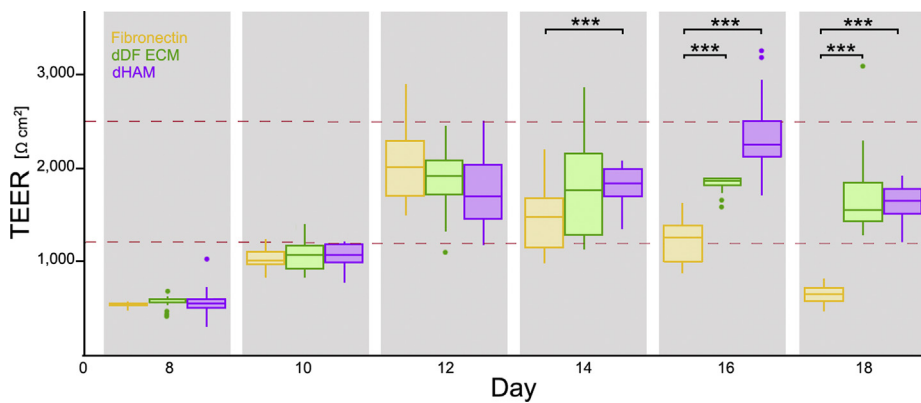
Figure 2. The TEER during HEE formation on different basement membrane substitutes. The TEER during HEE formation on fibronectin (orange), dDF ECM (green), and dHAM (purple) over a period of 18 days reflects permeability barrier formation (n = 12 for each condition; each point represents an average of measurements from three different spots). Values between 1,200–2,500 Ωcm^2 (red dashed line) indicated a formed permeability barrier. The TEER values of HEE cultured on dDF ECM and dHAM remained within the indicated standard, whereas the TEER values began declining after 14 days of culture on fibronectin. The data were analyzed using a two-sample Wilcoxon rank-sum (Mann–Whitney) test (***$P \leq 0.001$) and shown as a box plot of interquartile range and median values with outliers as dots. The confidence interval (95%) was calculated using the Bootstrap method. dDF ECM, decellularized dermal fibroblast–produced and –assembled extracellular matrix; dHAM, dry human amniotic membrane; HEE, human epidermal equivalent; TEER, transepithelial electrical resistance.

of 1,200–2,500 Ωcm^2 only for 3–4 days before starting to deteriorate, whereas HEEs cultured on dDF ECM or dHAM lasted up to 6 days before TEER became out of range (Figure 2).

Morphology and stratification of basal and suprabasal layers are not affected by the type of basement membrane substitutes

Following the parameters outlined in a consensus on the quality standard of organotypic models suitable for dermatological research (van den Bogard et al., 2021), next, we analyzed the morphology and stratification of the HEEs (Figure 3).

Expression of keratin (K) 10 (Figure 3a), K1 (Figure 3b), and desmocollin 1 (Figure 3c) in HEEs reflected the typical pattern of their expression in suprabasal layers of normal human skin. Desmosomes were also present in all conditions (Figure 3d).

Basal layers were negative for K1 and K10 (Figure 3a and b) and positive for ΔN TP63 (Figure 3e), K14 (Figure 3f), and proliferative cells (Figure 3g). The percentage of cells positive for the marker of proliferation MKI67 did not differ significantly among the three conditions (Figure 3h).

These data indicate that the morphology and stratification of basal and suprabasal layers might not be affected by the type of basement membrane substitutes.

Impact of basement membrane substitutes on epidermal permeability barrier

We examined the morphology and integrity of the stratum corneum and stratum granulosum on day 14 of the 3D cultures when TEER values were within the expected range of 1,200–2,500 Ωcm^2 in all the three culture conditions (Figure 2). There was no visible desquamation as seen by scanning electron microscopy (Figure 4a). Corneodesmosomes were detectable under all conditions (Figure 4b and c). Synthesized by the KCs in stratum granulosum and secreted through the lamellar bodies, corneodesmosin is incorporated into the desmoglea of the desmosomes shortly before their transformation into corneodesmosomes during cornification (Jonca et al., 2011). In normal human skin as well as in HEEs cultured on dDF ECM or dHAM, corneodesmosin is localized in the stratum corneum and is predominantly membrane bound, whereas in HEE cultured on fibronectin-coated surface, the majority of corneodesmosin was still granular and was retained in the stratum granulosum. However, quantitative electron microscopy analysis for corneodesmosome density did not show a significant difference among the three conditions (Figure 4d). Lipid processing was comparable with that of normal human skin in all HEEs, and the lamellar bodies were present under all the three culture conditions (Figure 4e–g). Calcium ion (Ca^{++}) gradient and lanthanum nitrate perfusion assays suggested that the epidermal permeability barrier is functional (Figure 4h and i).

Similarly to corneodesmosin, tight junction–specific protein TJP1 was predominantly distributed within the cytoplasm of stratum granulosum KCs in HEE cultured on fibronectin-coated surfaces, whereas in HEEs cultured on dDF ECM or dHAM, TJP1 was more prominent around the cell membrane, which is similar to its distribution in normal human skin (Figure 5a). On the other hand, intracellular localization of FLG was similar under all conditions tested (Figure 5b).

Figure 3. Quality assessment of general tissue structure. Markers of (**a–d**) suprabasal and (**e–g**) basal layers are present in HEE cultured under all three different substrates: fibronectin, dDF ECM, and dHAM at day 14 of 3D culture display a pattern that is comparable with that of normal human skin: (**a**) K10 (arrows, bar = 100 μm), (**b**) K1 (arrows, bar = 20 μm), (**c**) DSC1 (arrows, bar = 20 μm), (**d**) desmosomes (arrows, bar = 200 nm), (**e**) ΔN TP63 (arrows, bar = 20 μm), (**f**) MKI67 (arrows, bar = 20 μm), and (**h**) K14 (arrows, bar = 20 μm). (**g**) Percentage of cells in the basal layer that are positive for the marker of proliferation MKI67. The data were analyzed using of one-way ANOVA test and shown as a box plot of interquartile range and median values. The statistical analysis has shown that there was no statistically significant difference in the percentage of MKI67+ among the groups (F[2, 42] = 0.028, *P* = 0.973). Tukey's HSD test for multiple comparisons did not detect any significant differences between pairs of groups: fibronectin versus dDF ECM (*P* = 0.977), fibronectin versus dHAM (*P* = 0.977), and dDF ECM versus dHAM (*P* = 1.000). The confidence interval (95%) was calculated using the Bootstrap method. 3D, three-dimensional; d, dermis; dDF ECM, decellularized dermal fibroblast–produced and – assembled extracellular matrix; dHAM, dry human amniotic membrane; DSC1, desmocollin 1; HEE, human epidermal equivalent; HSD, honestly significant difference; K, keratin; SB, stratum basale; SC, stratum corneum; SG, stratum granulosum; SS, stratum spinosum; TM, Transwell membrane.
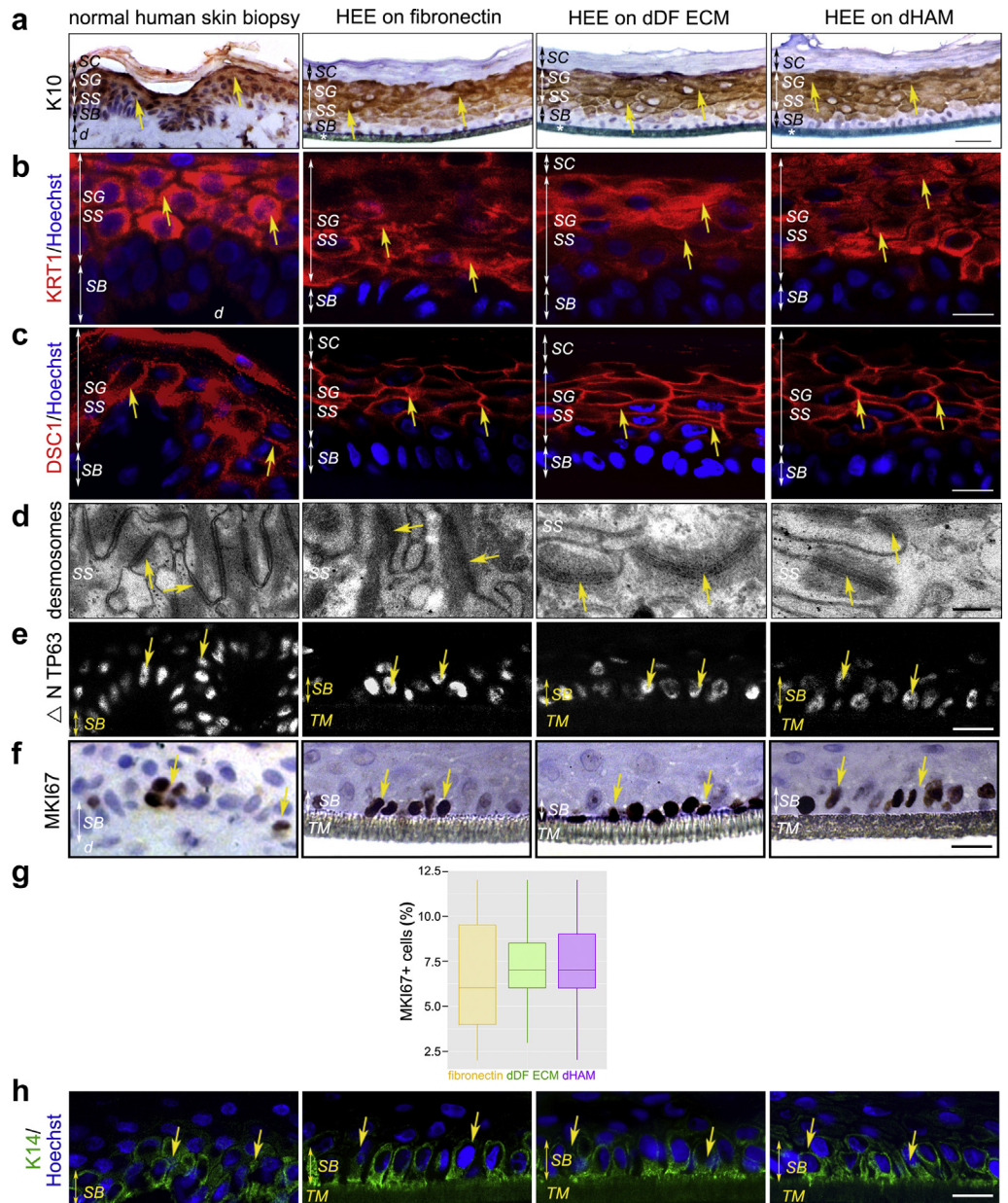
Impact of basement membrane substitutes on the composition of ECM in HEEs

Integrin β1 is considered a marker of KC stem cells in the basal layer (Zhu et al., 1999). Using mAb 9EG7 that recognizes an activation epitope on integrin beta1 (Lenter et al., 1993), we found no difference in the pattern between normal human skin and HEEs (Figure 6).

Next, we assessed ECM composition by immunostaining for collagen IV, collagen VI, and collagen VII, and laminin-5 (Figure 6). Although all the four proteins were detected on the surface of Transwell inserts with dDF ECM and dHAM basement membrane substitutes, we did not detect collagen VI in HEE cultures on fibronectin-coated inserts. Furthermore, collagen IV, collagen VII, and laminin-5 were more abundant in HEE cultures on dDF ECM or dHAM basement membrane substitutes than on fibronectin-coated inserts.

Complex 3D basement membrane substitutes, dDF ECM and dHAM, support the formation of hemidesmosomes in HEE

We used transmission electron microscopy to evaluate whether the composition of the ECM detected in basement membrane substitutes had any effect on the structural morphology of KCs in the basal layer. We found that dDF ECM and dHAM supported the formation of hemidesmosomes, whereas fibronectin coating did not (Figure 7). We did not find a significant difference in the number of hemidesmosomes formed over a specific length of the cell membrane proximal to the basement membrane substitute in the HEE cultured on dDF ECM (4.36 ± 1.08 per 1 μM) or dHAM (4.36 ± 1.21 per 1 μM) (Figure 7c). The size of hemidesmosomes was also similar (178.40 ± 4.98 in HEE cultured on dDF ECM and 179.80 ± 7.57 in HEE cultured on dHAM) (Figure 7d). The data support our hypothesis that
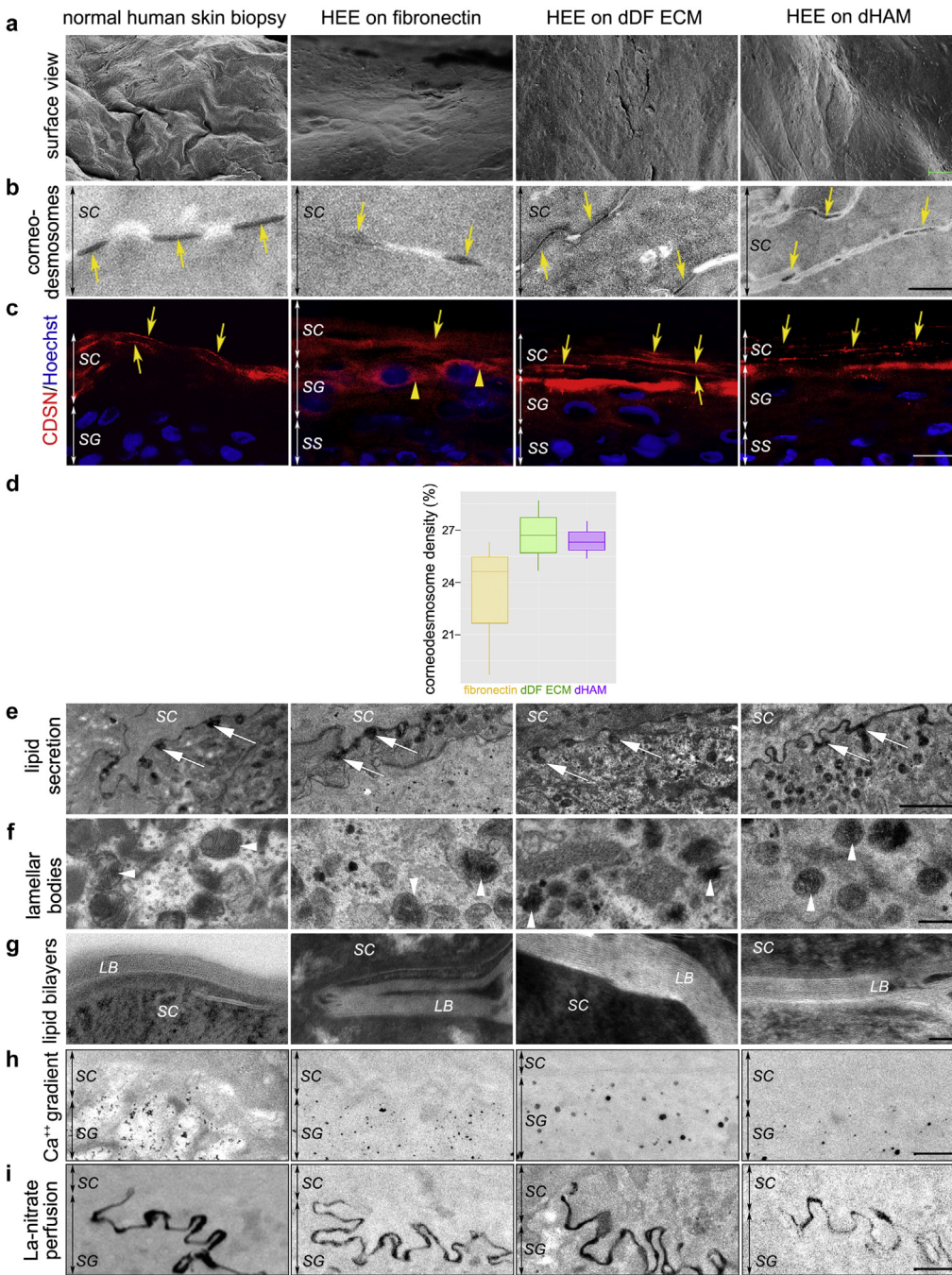
Figure 4. Quality assessment of epidermal permeability barrier. HEE on fibronectin, dDF ECM, and dHAM demonstrate permeability barrier formation. (**a**) Scanning electron microscopy images of human skin and HEEs. Bar = 20 μm. (**b**) Corneodesmosomes (arrows) were present in all HEEs. Bar = 0.5 μm. (**c**) In HEE grown on fibronectin, CDSN pattern was more cytoplasmic (arrowheads) than membrane bound (arrows). Bar = 20 μm. (**d**) Quantitative electron microscopy analysis for corneodesmosome density. The data were analyzed using of one-way ANOVA test and shown as a box plot of interquartile range and median values. The statistical analysis revealed that there was no statistically significant difference in desmosome density between at least two groups (F [2, 6] = 1.611, P = 0.275), even though it looks like HEEs cultured on fibronectin have a smaller median. Similarly, Kruskal–Wallis rank-sum test shows the same lack of overall significance of corneodesmosome density (H = 2.89, df = 2, P = 0.236). There was no statistically significant difference between the condition seen by Tukey's HSD test: fibronectin versus dDF ECM (P = 0.309), fibronectin versus dHAM (P = 0.364), and dDF ECM versus dHAM (P = 0.990). Confidence interval (95%) was calculated using the Bootstrap method. (**e–g**) Lipid processing has been detected in all HEEs. Bar = 1 μm for **e**, 200 nm for **f**, and 50 nm for **g**. (**h**) Ca^{++} were detected in SG and not in SC of HEEs. Bar = 0.5 μm. (**i**) Lanthanum nitrate perfusion assay showed tight junctions integrity and barrier function in all HEEs. Bar = 0.5 μm. Ca^{++}, calcium ion; CDSN, corneodesmosin; dDF ECM, decellularized dermal fibroblast–produced and –assembled extracellular matrix; dHAM, dry human amniotic membrane; HEE, human epidermal equivalent; HSD, honestly significant difference; LB, lipid bilayer; SC, stratum corneum; SG, stratum granulosum; SS, stratum spinosum.

more precise mimicking of the basement membrane could improve the quality of the bioengineered HEEs as in this example where dDF ECM and dHAM facilitated the formation of hemidesmosomes.

DISCUSSION

Organotypic cultures of human skin or reconstructed human skin equivalents (HSEs) are widely used in basic and translational research. Quite often, such complex models are not needed, and the research questions, especially those related to the epidermal permeability barrier, can be addressed using much simpler models such as HEEs. HEEs can be bioengineered faster than HSEs; however, they have the disadvantage of being short lived. Whereas HSEs can be maintained for several months in the culture, fully stratified functional HEEs deteriorate in a few days.

A small difference in culture conditions, in the composition of culture media, as well as in genetic

Figure 5. Quality assessment of SG. (**a**) In HEE grown on fibronectin, TJP1 pattern was more cytoplasmic (arrowheads) than membrane bound (arrows). Bar = 20 μm. (**b**) FLG-positive granules were detected in all the HEE. Bar = 20 μm. dHAM, dry human amniotic membrane; HEE, human epidermal equivalent; SC, stratum corneum; SG, stratum granulosum; SS, stratum spinosum.
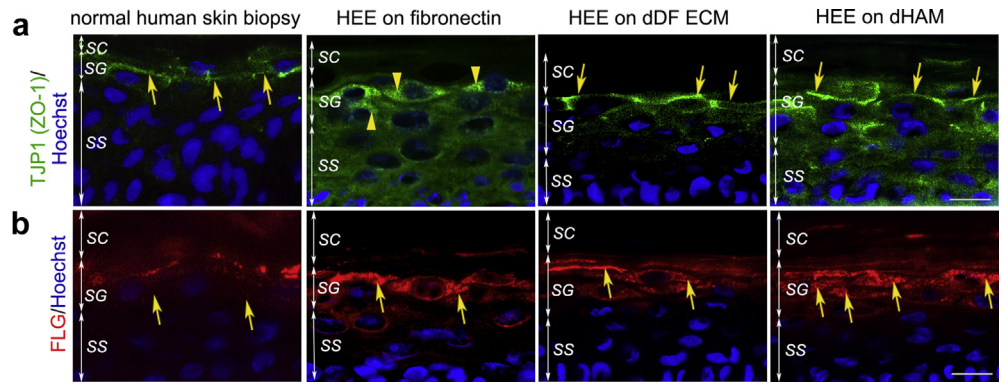
polymorphism and other variabilities between donors could affect the quality of both HSEs and HEEs and easily result in misinterpretation of the data. A consensus opinion on quality standard and validation of models suitable for research has been recently published (van den Bogard et al., 2021).

We followed the guidelines and used the recommended validation parameters for quality assessment of general tissue structure and some parameters specific to epidermal permeability barrier to determine whether complex 3D basement membrane substitutes, such as Matrigel, dDF ECM, and dHAM, provide any advantage for the quality of HEEs.

Our data suggest several conclusions: (i) differentiation and stratification of KCs in 3D culture are dependent on the substrate on which the cells were plated, (ii) HEE longevity is also affected by the substrate on which the cells were plated, and (iii) dDF ECM and dHAM but not Matrigel or fibronectin support the formation of hemidesmosomes in HEEs without the need for dermal components in HSE.

Figure 6. BM substitutes and ECM expression. Expression of integrin β1 and ECM proteins in normal human skin and HEEs cultured on three different substrates. Red arrowheads indicate the positive signal in the d. Red arrows indicate the positive signal in keratinocytes. Bar = 20 μm. BM, basement membrane; d, dermis; dDF ECM, decellularized dermal fibroblast–produced and –assembled extracellular matrix; e, epidermis; ECM, extracellular matrix; HEE, human epidermal equivalent; SB, stratum basale; SG, stratum granulosum; SS, stratum spinosum; TM, Transwell membrane.
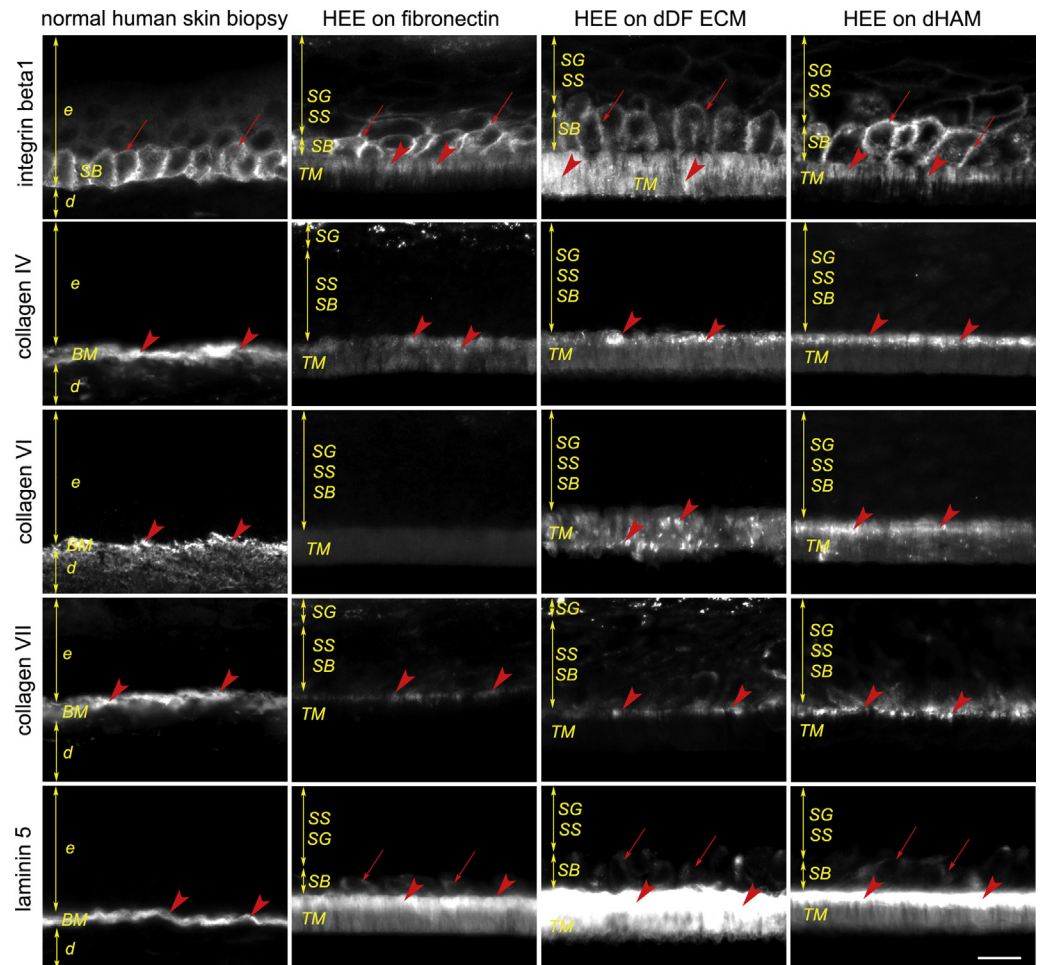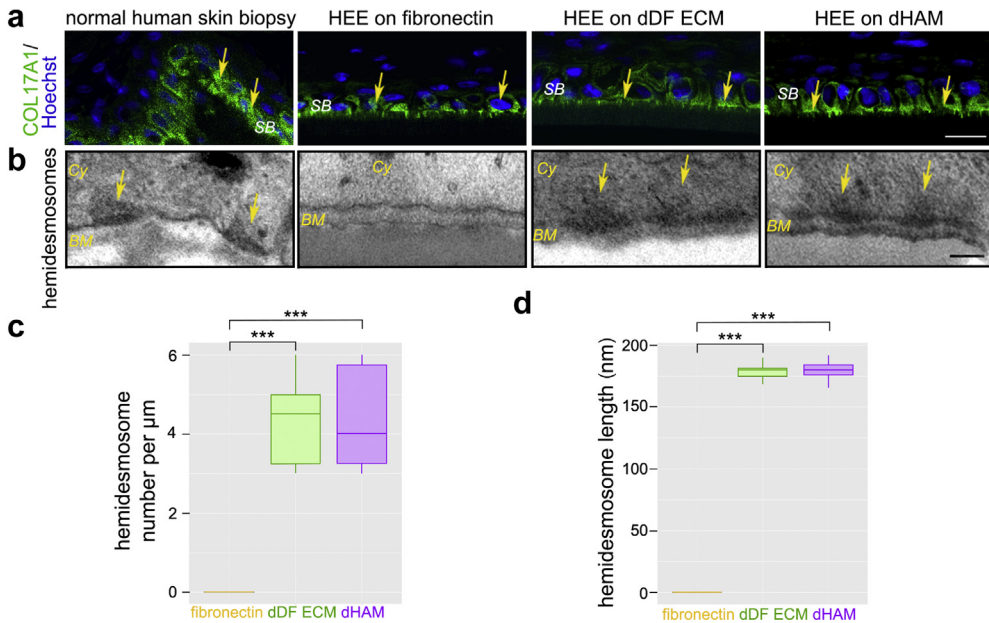
Figure 7. dDF ECM and dHAM support the formation of hemidesmosomes, whereas fibronectin-coated surface does not. (**a**) COL17A1 (arrows) was detected in cells of SB under all conditions. Bar = 20 μm. (**b**) Hemidesmosomes were detected by transmission electron microscopy in HEE cultured on dDF ECM and dHAM. Yellow arrows indicate hemidesmosomes. Bar = 150 nm. (**c**) Number of hemidesmosomes over a specific length of the cell membrane proximal to the basement membrane substitute. The data were analyzed using of one-way ANOVA test and shown as a box plot of interquartile range and median values. The results showed a statistically highly significant difference in response variable between at least two groups ($F[2,39] = 100.4$, $P = 4.18e-16$). Tukey's HSD test revealed that the mean value of hemidesmosome density was significantly different between HEEs cultured on dDF ECM and fibronectin and between HEEs cultured on dHAM and fibronectin (***$P \leq 0.001$). Confidence interval (95%) was calculated using the Bootstrap method. (**d**) Size of hemidesmosomes. The data were analyzed using of one-way ANOVA test and shown as a box plot of interquartile range and median values. Tukey's HSD test for multiple comparisons revealed that the mean value of the hemidesmosome length was significantly different between HEEs cultured on dDF ECM and fibronectin and also between HEEs cultured on dHAM and fibronectin (***$P \leq 0.001$). Confidence interval (95%) was calculated using the Bootstrap method. BM, basement membrane; Cy, cytoplasm; dDF ECM, decellularized dermal fibroblast–produced and –assembled extracellular matrix; dHAM, dry human amniotic membrane; HEE, human epidermal equivalent; HSD, honestly significant difference; SB, stratum basale.

Differentiation and stratification of HEE are dependent on the substrate on which the cells were plated

Matrigel, a basement membrane equivalent, is widely used as a substrate for various cell types, including human pluripotent stem cells. In dermatological research, Matrigel was used for a culture of hair follicle KCs (Havlickova et al., 2004; Limat et al., 1994; Miao et al., 2014; Oh et al., 2011) as well as of primary human KCs (Saarialho-Kere et al., 1993). However, it did not support the stratification of the HaCaT cells (Coelho-Sampaio et al., 2020). On the other hand, fibronectin (Petrova et al., 2016, 2014; Sun et al., 2015) or collagen I (Rikken et al., 2020), which

are not basement membrane constituents, did support stratification.

The signals from the ECM that govern KC stratification are still unknown; more research is needed to enable successful bioengineering of HEEs with ECM and basement membrane substitutes.

HEE longevity is affected by the basement membrane substitute on which the cells were plated

HSEs could be maintained in the culture for weeks (El Ghalbzouri et al., 2009), whereas the lifespan of HEEs is much shorter (Petrova et al., 2016, 2014; Sun et al., 2015).

Rapid turnover of KC stem cells in the basal layer of the epidermis is required for the homeostasis of the epidermis (or HEEs). Terminal differentiation in the upper layers of the epidermis triggers differentiation and delamination in the basal layer, liberating space. This alters the basal cell size of the neighboring cells, triggering cell division of the largest cell to restore homeostatic cell density (Mesa et al., 2018). The signals that maintain their stemness are coming from the stem cell niche (Chacón-Martínez et al., 2018; Lane et al., 2014). ECM receptor, integrin β1, is considered as a marker of KC stem cells in the basal layer (Zhu et al., 1999); It is plausible to hypothesize that the right composition of the ECM might provide the required signals for the maintenance of their stemness. However, the integrins are also mechano-receptors, and they are tightly linked with GF signaling (Damsky and Ilić, 2002, 2002; Sieg et al., 2000).

Although the two basement membrane substitutes that we tested did extend the lifespan of HEEs (Figure 2), they do not provide the ultimate answer. The ECM is not the sole component of the stem cell niche. Various soluble components (e.g., GF, cytokines), physical factors (e.g., stiffness, topography), or metabolic factors (e.g., oxygen, Ca^{++}) as well as cellular components (e.g., cell–cell contacts) play an integral role in the interaction between stem cells and their niche. This interaction is complex, bidirectional, and reciprocal (Lane et al., 2014).

dDF ECM and dHAM but not Matrigel or fibronectin support the formation of hemidesmosomes in HEEs

Hemidesmosomes are highly specialized integrin-mediated epithelial-attachment structures that link the underlying basement membrane and the internal keratin intermediate filament network. Owing to the lack of a suitable in vitro model, they have been mostly studied in vivo. Several lines of evidence suggest that the binding of α6β4 integrin to laminin-322 is a crucial step in hemidesmosome assembly (Walko et al., 2015). It might be that laminin-322 was present in both dDF ECM and dHAM and that that was sufficient to trigger the formation of hemidesmosomes. Although we did not detect clear differences in the immunostaining pattern of COL17A1 (Figure 7a), we cannot exclude the possibility that the signals from dDF ECM and dHAM triggered the expression of some other structural component(s) otherwise missing in the basal layer KCs.

Importance of 3D structure of the ECM

The importance of 3D ECM has been recognized for epithelial cells, where 3D environments and a continuous flow of information between cells and the ECM regulate normal epithelial polarity and differentiation (Roskelley et al., 1995). A few years later, Kenneth Yamada's group demonstrated that relative to that of two-dimensional substrates, 3D–matrix interactions display enhanced biological activities (Cukierman et al., 2001). The 3D–matrix adhesions differ in structure, molecular composition, localization, and function from the adhesions formed on two-dimensional substrates such as fibronectin coating. Similarly, 3D substrates that we used to mimic basement membrane may be more biologically relevant to living organisms than standard two-dimensional fibronectin coating and as such promote the formation of hemidesmosomes.

The results of this study indicate that more suitable basement membrane substitutes, such as dDF ECM and dHAM, can better support the structural and functional integrity of HEEs. The ability to assemble hemidesmosomes in a simple model will allow for further studies on epidermal homeostasis and the biology of the dermal–epidermal junction and for a better understanding of how dysfunction of these components leads to diseases such as non-Herlitz junctional epidermolysis bullosa and epithelial recurrent erosion dystrophy.

MATERIALS AND METHODS

Cells

Primary normal human KCs were isolated from neonatal foreskins and expanded in 0.07 mM Ca^{++} 154CF medium (Thermo Fisher Scientific, Waltham, MA) with a human KC growth supplement. Isolation and culture of primary normal human KCs from neonatal foreskin has been approved by the University of California San Francisco (San Francisco, CA) Institutional Review Board (#10-00944). The foreskin of circumcised newborn boys was obtained following parental written informed consent.

Preparation of basement membrane substitutes

For 3D culture, we used 12 mm Transwells with 0.4-μm pore polycarbonate membrane insert (Millipore, Burlington, MA).

For fibronectin, the insert was coated with CELLstart (Thermo Fisher Scientific) for 1 hour at 37 °C according to the manufacturer's instructions.

For dDF ECM, dDF ECM was prepared as described previously (Ilic et al., 2012). Dermal fibroblasts were mitotically inactivated with γ-irradiation at 5,000 rad (50 Gy) with a cesium-source irradiator GammaCell 100 Elite (Nordion International, Ontario, Canada), and 36,000 cells/cm2 were plated in a chemically defined, xeno-free CnT-PR-ECM medium (CELLnTEC Advanced Cell Systems, Bern, Switzerland) for a minimum of 7 days. The medium was changed daily. The dermal fibroblasts were lysed in 0.5% (v/v) Triton X-100 and 20 mM ammonium hydroxide in PBS for 5 minutes. The remaining dDF ECM was gently rinsed at least three times with PBS and used either immediately or stored at 4 °C for up to 1 week.

For dHAM, Amniomatrix membrane (Next Biosciences, Midrand, South Africa) was cut into $\approx 1.2 \times 1.2$ cm^2 squares, and one square was placed on the bottom of each insert. To adhere dHAM to the bottom and the sides of the insert, we added 100–200 μl of culture medium for 10 minutes.

HEEs

Normal human KCs ($\approx 250,000$/cm^2) were plated into inserts either coated with CELLstart only or having either dDF ECM or dHAM at the bottom. The cells were cultured as described previously (Petrova et al., 2016, 2014; Sun et al., 2015). The experiment has been repeated three times, each with a different batch of primary KCs that were pooled from five different donors. For each round of the experiments, we set a 12-well plate with Transwell inserts, four insets per each of the three conditions (fibronectin coated, dDF ECM, and dHAM). On day 14, the membranes with HEE were cut out from the insets and processed for immunostaining or electron microscopy for morphological or functional evaluation. Images presented in the manuscript are representative images from three independent experiments.

Immunolocalization

Cryosections. The samples were fixed in 3.8% para-formaldehyde/PBS at pH 7.2–7.6 for 30 minutes, washed three times

for 5 minutes in PBS, and infiltrated with a series of sterile sucrose gradients (10% sucrose overnight, 15% sucrose for 6–8 hours, 30% sucrose overnight, and finally 30% sucrose mixed at 1:1 with optimal cutting temperature compound overnight) rotating on 4 °C. The samples were finally embedded in optimal cutting temperature and frozen in liquid nitrogen vapor. The cryoblocks were stored at −80 °C. The day before cutting, the cryoblocks were transferred to −20 °C overnight. Sections (10-μm tick) were prepared using a standard cryostat. The sections were kept at −20 °C till processing.

The sections were submerged in either 90% cold acetone for 10 minutes or 0.2% Triton X-100/PBS for 5 minutes to expose antigens. The samples were washed three times for 5 minutes in PBS. The sections were then incubated overnight at 4 °C with a mixture of the following two antibodies: (i) 2.5 μg/ml of ChromPure donkey whole IgG (for purpose of blocking, all secondary antibodies are made in donkey) and (ii) 1 μg/ml of appropriate primary antibody. The sections were rinsed three times for 5 minutes in PBS; incubated for 20 minutes at room temperature with 10 μg/ml Hoechst 33342 (Thermo Fisher Scientific) and the appropriate species-specific secondary antibody, made in donkey; and conjugated to either red or green fluorophore. The sections were washed three times for 5 minutes in PBS, mounted with Vectashield medium (Vector Laboratories, Burlingame, CA) and with an epifluorescence microscope (Carl Zeiss, Jena, Germany), equipped with appropriate filters.

For control incubations, preimmune sera or isotype-matched nonimmune antibodies were used instead of the primary antibodies. Staining of control tissue sections was never observed (data not shown).

Paraffin-embedded sections. For paraffin-embedded sections, the samples were fixed in 3.8% paraformaldehyde/PBS at pH 7.2–7.6 for 30 minutes, washed three times 5 minutes in PBS, and dehydrated in ascending ethanol series (50, 70, and twice for 100%; 20 minutes each) and clearing agent (xylene, two times for 20 minutes). The samples were perfused with paraffin wax at 65 °C two times for 1 hour and embedded in paraffin blocks. The paraffin blocks were stored at room temperature until further use. The tissue was sectioned at 5-μm thickness using a standard microtome. The sections were kept at room temperature till processing.

The sections were rehydrated in ascending xylene/ethanol series (twice for xylene, twice for 100% ethanol, and once for 70 and 50%, 10 minutes each); briefly rinsed with tap water; and then stained with hematoxylin for 5 minutes, washed with deionized water until the solution was clear, and stained with 0.5% eosin for 10 minutes and rinsed briefly in tap water.

The sections were then incubated overnight at 4 °C with a mixture of the following two antibodies: (i) 2.5 μg/ml of ChromPure donkey whole IgG (for purpose of blocking, all secondary antibodies are made in donkey) and (ii) 1 μg/ml of appropriate primary antibody. The sections were rinsed three times for 5 minutes in PBS; incubated for 20 minutes at room temperature with the appropriate species-specific secondary antibody, made in donkey; and conjugated to horseradish peroxidase. The sections were washed three times for 5 minutes in PBS.

For visualization, the samples were incubated with a 3, 3′-diaminobenzidine substrate kit (Vector Laboratories) according to the manufacturer's instructions. The 3, 3′-diaminobenzidine will yield a brown stain. If nickel chloride is added to the substrate solution, a gray–black stain will result. The samples were dehydrated in ascending ethanol series (50, 70, and twice for 100%, 10 minutes each) and clearing agent (xylene, twice for 10 minutes), mounted in

mounting medium, and visualized with a phase-contrast microscope (Carl Zeiss) equipped with a digital camera.

For control incubations, preimmune sera or isotype-matched nonimmune antibodies were used instead of the primary antibodies. Staining of control tissue sections was never observed (data not shown).

TEER

TEER was measured at three different points in each of HEEs at the indicated days using EVOM voltohmmeter (World Precision Instruments, Sarasota, FL). The Transwell membrane resistance (100 Ωcm^2) was subtracted from each measurement, and the value was multiplied with the surface area of the Transwell (1.12 cm^2).

Field emission scanning electron microscopy

The samples were fixed for 30 minutes at 4 °C with 4% paraformaldehyde and 2% glutaraldehyde in 0.1 M sodium cacodylate buffer (pH 7.4) and stored in 0.1 M sodium cacodylate buffer at 4 °C before further processing.

The samples were post fixed for 1 hour with 1% aqueous osmium tetroxide. After dehydration in an ascending ethanol series (50, 70, and twice for 100%, 10 minutes each), samples were critical point dried with liquid carbon dioxide in a Tousimis Autosamdri-815B apparatus (Tousimis Research, Rockville, MA), mounted with double-sided copper tape onto 15 mm aluminum mounts, and sputter coated with 40 Å of gold-palladium using a Denton DeskII Sputter Coater (Denton Vacuum, Moorestown, NJ).

Cross-sections of duplicate samples were mounted onto low-profile 45/90degree scanning electron microscopy mounts for analysis of internal morphology. Visualization was performed with a Zeiss Sigma Field Emission Scanning Electron Microscope (Carl Zeiss Microscope) operated at 2–3 kV, using InLens Secondary Electron detection, as well as mixed-signal InLens/SE2 (75/25%) detection at a working distance of 3–5 mm. Images were captured in TIFF using a store resolution of 2,048 × 1,536 and a line averaging noise reduction algorithm.

Transmission electron microscopy

The samples were fixed for 30 minutes at 4 °C with 4% paraformaldehyde and 2% glutaraldehyde in 0.1 M sodium cacodylate buffer (pH 7.4) and stored in 0.1 M sodium cacodylate buffer at 4 °C before further processing.

The samples were then washed and placed in either 0.2% ruthenium tetroxide (for visualization of lipid bilayers) or 1.5% osmium tetroxide with 1.5% potassium ferrocyanide, in 0.1 M sodium cacodylate, at pH 7.4, and at room temperature in the dark for 45 minutes. After rinsing in buffer, the samples were dehydrated in a graded ethanol series (50, 70, and twice for 100%, 10 minutes each) and were subsequently embedded in a low-viscosity, Epoxy resin.

Semithin sections were stained with 1% toluidine blue with 1% azure II in 1% borax solutions and viewed under a phase-contrast microscope (Carls Zeiss).

Ultrathin sections were collected and stained with water-saturated 3% uranyl acetate and/or contrasted in 2.5% lead citrate on uncoated nickel grids. Ultrathin sections were viewed with a Zeiss 10 A electron microscope operated at 60 kV. Images were captured in TIFF.

Ion capture cytochemistry (Ca^{++} gradient)

For ultrastructural Ca^{++} localization, the samples were fixed in 2% paraformaldehyde, 2% glutaraldehyde, and 0.09 M potassium oxalate containing 0.04 M sucrose. Samples were subsequently fixed overnight at 4 °C.

The samples were post fixed in 1% osmium tetroxide containing 2% potassium pyroantimonate at pH 7.4 for 2 hours at 4 °C in the dark. Tissue samples then were washed in alkalinized water (pH 10) and transferred to ethanol solutions (50, 70, twice for 100%, 10 minutes each) for dehydration and embedding in a low-viscosity, Epoxy resin.

Ultrathin sections were collected and stained with water-saturated 3% uranyl acetate and/or contrasted in 2.5% lead citrate on un-coated nickel grids. Ultrathin sections were viewed with a Zeiss 10 A electron microscope operated at 60 kV. Images were captured in TIFF.

Lanthanum perfusion

The perfusion pathway was assessed by placing the HEE samples on a drop of 4% lanthanum nitrate in 0.05 M Tris buffer containing 2% glutaraldehyde and 1% paraformaldehyde at pH 7.4 for 1 hour at room temperature.

The samples were washed and placed in 1.5% osmium tetroxide with 1.5% potassium ferrocyanide in 0.1 M sodium cacodylate at pH 7.4 at room temperature in the dark for 45 minutes. After rinsing in cacodylate buffer, the samples were dehydrated in a graded ethanol series (50, 70, twice for 100%, 10 minutes each) and were subsequently embedded in a low-viscosity, Epoxy resin.

Ultrathin sections were collected and stained with water-saturated 3% uranyl acetate and/or contrasted in 2.5% lead citrate on un-coated nickel grids. Ultrathin sections were viewed with a Zeiss 10 A electron microscope operated at 60 kV. Images were captured in TIFF.

Data availability statement

There are no data sets used in the preparation of this article.

ORCIDs

Nikola Kolundzic: http://orcid.org/0000-0002-6480-2729
Preeti Khurana: http://orcid.org/0000-0002-0252-9819
Debra Crumrine: http://orcid.org/0000-0002-8492-5670
Anna Celli: http://orcid.org/0000-0002-0605-0362
Theodora M. Mauro: http://orcid.org/0000-0003-3623-0070
Dusko Ilic: http://orcid.org/0000-0003-1647-0026

CONFLICT OF INTEREST

The authors state no conflict of interest.

REFERENCES

Borries M, Barooji YF, Yennek S, Grapin-Botton A, Berg-Sørensen K, Oddershede LB. Quantification of visco-elastic properties of a matrigel for organoid development as a function of polymer concentration. Front Phys 2020;8:579168.

Bourne GL. The microscopic anatomy of the human amnion and chorion. Am J Obstet Gynecol 1960;79:1070−3.

Chacón-Martínez CA, Koester J, Wickström SA. Signaling in the stem cell niche: regulating cell fate, function and plasticity. Development 2018;145: dev165399.

Coelho-Sampaio T, Tenchov B, Nascimento MA, Hochman-Mendez C, Morandi V, Caarls MB, et al. Type IV collagen conforms to the organization of polylaminin adsorbed on planar substrata. Acta Biomater 2020;111: 242−53.

Cruz-Acuña R, García AJ. Synthetic hydrogels mimicking basement membrane matrices to promote cell-matrix interactions. Matrix Biol 2017;57−58:324−33.

Cukierman E, Pankov R, Stevens DR, Yamada KM. Taking cell-matrix adhesions to the third dimension. Science 2001;294:1708−12.

Damsky CH, Ilić D. Integrin signaling: it's where the action is. Curr Opin Cell Biol 2002;14:594−602.

Dietrich-Ntoukas T, Hofmann-Rummelt C, Kruse FE, Schlötzer-Schrehardt U. Comparative analysis of the basement membrane composition of the human limbus epithelium and amniotic membrane epithelium. Cornea 2012;31:564−9.

El Ghalbzouri A, Commandeur S, Rietveld MH, Mulder AA, Willemze R. Replacement of animal-derived collagen matrix by human fibroblast-derived dermal matrix for human skin equivalent products. Biomaterials 2009;30:71−8.

Gindraux F, Laurent R, Nicod L, de Billy B, Meyer C, Zwetyenga N, et al. Human amniotic membrane: clinical uses, patents and marketed products. Rec Pat Regen Med 2013;3:193−214.

Havlickova B, Bíró T, Mescalchin A, Arenberger P, Paus R. Towards optimization of an organotypic assay system that imitates human hair follicle-like epithelial-mesenchymal interactions. Br J Dermatol 2004;151:753−65.

Ilic D, Stephenson E, Wood V, Jacquet L, Stevenson D, Petrova A, et al. Derivation and feeder-free propagation of human embryonic stem cells under xeno-free conditions. Cytotherapy 2012;14:122−8.

Ilic D, Vicovac L, Nikolic M, Lazic Ilic E. Human amniotic membrane grafts in therapy of chronic non-healing wounds. Br Med Bull 2016;117: 59−67.

Jonca N, Leclerc EA, Caubet C, Simon M, Guerrin M, Serre G. Corneo-desmosomes and corneodesmosin: from the stratum corneum cohesion to the pathophysiology of genodermatoses. Eur J Dermatol 2011;21(Suppl. 2): 35−42.

Khurana P, Kolundzic N, Flohr C, Ilic D. Human pluripotent stem cells: an alternative for 3D in vitro modelling of skin disease. Exp Dermatol 2021;30:1572−87.

Koizumi NJ, Inatomi TJ, Sotozono CJ, Fullwood NJ, Quantock AJ, Kinoshita S. Growth factor mRNA and protein in preserved human amniotic membrane. Curr Eye Res 2000;20:173−7.

Koob TJ, Lim JJ, Massee M, Zabek N, Denozière G. Properties of dehydrated human amnion/chorion composite grafts: implications for wound repair and soft tissue regeneration. J Biomed Mater Res B Appl Biomater 2014;102:1353−62.

Lane SW, Williams DA, Watt FM. Modulating the stem cell niche for tissue regeneration. Nat Biotechnol 2014;32:795−803.

Lenter M, Uhlig H, Hamann A, Jenö P, Imhof B, Vestweber D. A monoclonal antibody against an activation epitope on mouse integrin chain beta 1 blocks adhesion of lymphocytes to the endothelial integrin alpha 6 beta 1. Proc Natl Acad Sci USA 1993;90:9051−5.

Limat A, Breitkreutz D, Hunziker T, Klein CE, Noser F, Fusenig NE, et al. Outer root sheath (ORS) cells organize into epidermoid cyst-like spheroids when cultured inside Matrigel: a light-microscopic and immunohistological comparison between human ORS cells and interfollicular keratinocytes. Cell Tissue Res 1994;275:169−76.

Mesa KR, Kawaguchi K, Cockburn K, Gonzalez D, Boucher J, Xin T, et al. Homeostatic epidermal stem cell self-renewal is driven by local differentiation. Cell Stem Cell 2018;23:677−86.e4.

Miao Y, Sun YB, Liu BC, Jiang JD, Hu ZQ. Controllable production of transplantable adult human high-passage dermal papilla spheroids using 3D matrigel culture. Tissue Eng Part A 2014;20:2329−38.

Oh JH, Mohebi P, Farkas DL, Tajbakhsh J. Towards expansion of human hair follicle stem cells in vitro. Cell Prolif 2011;44:244−53.

Petrova A, Capalbo A, Jacquet L, Hazelwood-Smith S, Dafou D, Hobbs C, et al. Induced pluripotent stem cell differentiation and three-dimensional tissue formation attenuate clonal epigenetic differences in trichohyalin. Stem Cells Dev 2016;25:1366−75.

Petrova A, Celli A, Jacquet L, Dafou D, Crumrine D, Hupe M, et al. 3D in vitro model of a functional epidermal permeability barrier from human embryonic stem cells and induced pluripotent stem cells. Stem Cell Rep 2014;2:675−89.

Pozzi A, Yurchenco PD, Iozzo RV. The nature and biology of basement membranes. Matrix Biol 2017;57−58:1−11.

Randles MJ, Humphries MJ, Lennon R. Proteomic definitions of basement membrane composition in health and disease. Matrix Biol 2017;57—58:12—28.

Rikken G, Niehues H, van den Bogaard EH. Organotypic 3D skin models: human epidermal equivalent cultures from primary keratinocytes and immortalized keratinocyte cell lines. Methods Mol Biol 2020;2154:45—61.

Roig-Rosello E, Rousselle P. The human epidermal basement membrane: a shaped and cell instructive platform that aging slowly alters. Biomolecules 2020;10:1067.

Roskelley CD, Srebrow A, Bissell MJ. A hierarchy of ECM-mediated signalling regulates tissue-specific gene expression. Curr Opin Cell Biol 1995;7:736—47.

Saarialho-Kere UK, Kovacs SO, Pentland AP, Olerud JE, Welgus HG, Parks WC. Cell-matrix interactions modulate interstitial collagenase expression by human keratinocytes actively involved in wound healing. J Clin Invest 1993;92:2858—66.

Sieg DJ, Hauck CR, Ilic D, Klingbeil CK, Schaefer E, Damsky CH, et al. FAK integrates growth-factor and integrin signals to promote cell migration. Nat Cell Biol 2000;2:249—56.

Sun R, Celli A, Crumrine D, Hupe M, Adame LC, Pennypacker SD, et al. Lowered humidity produces human epidermal equivalents with enhanced barrier properties. Tissue Eng Part C Methods 2015;21:15—22.

Uchida Y, Celli A. A method to investigate the epidermal permeability barrier in vitro. Methods Mol Biol 2020;2154:73—90.

van den Bogaard E, Ilic D, Dubrac S, Tomic-Canic M, Bouwstra J, Celli A, et al. Perspective and consensus opinion: good practices for using organotypic skin and epidermal equivalents in experimental dermatology research [published correction appears in J Invest Dermatol 2021;141:1862]. J Invest Dermatol 2021;141:203—5.

van Herendael BJ, Oberti C, Brosens I. Microanatomy of the human amniotic membranes. A light microscopic, transmission, and scanning electron microscopic study. Am J Obstet Gynecol 1978;131:872—80.

Walko G, Castañón MJ, Wiche G. Molecular architecture and function of the hemidesmosome. Cell Tissue Res 2015;360:363—78.

Zhang Z, Li Z, Li Y, Wang Y, Yao M, Zhang K, et al. Sodium alginate/collagen hydrogel loaded with human umbilical cord mesenchymal stem cells promotes wound healing and skin remodeling. Cell Tissue Res 2021;383:809—21.

Zhu AJ, Haase I, Watt FM. Signaling via beta1 integrins and mitogen-activated protein kinase determines human epidermal stem cell fate in vitro. Proc Natl Acad Sci USA 1999;96:6728—33.